Research Article

Investigation of a Mathematical Model and Non-Linear Effects Based on Parallel-Substrates Biochemical Conversion

Nebiyal A[1]*[ID], Swaminathan R[1], Raja R[2, 3], Karpagavalli SG[1]

[1] PG and Research Department of Mathematics, Vidhyaa Giri College of Arts and Science, Affiliated to Alagappa University, Sivaganga-630108, India
[2] Ramanujan Centre for Higher Mathematics, Alagappa University, Karaikudi, India
[3] Department of Computer Science and Mathematics, Lebanese American University, Beirut, Lebanon
 E-mail: sgkarpa@gmail.com

Abstract: According to the broad applicability and advancements made in addressing complex non-linear problems, Researchers have been actively involved in addressing the accurate approaches to solve non-linear problems in fields such as chemical science, material science, and image processing. In this paper, the Amperometric response of catalase-peroxidase (parallel-substrates) conversion has been discussed. The Mathematical model relies on a set of non-linear differential equations that describe the reaction and diffusion of the system. The analytical methods were extended to derive the approximate solution of the non-linear reaction-diffusion equation. The straightforward and concise analytical expressions for the concentrations and current of the Biosensor are developed. This study includes the computational resolution of the problem by utilizing a MATLAB program. A comparison between analytical outcomes and those derived numerically has been conducted. The analytical findings presented are dependable and offer an effective comprehension of the behaviour of this system.

Keywords: mathematical modelling, Akbari-Ganji's method (AGM), differential transform method (DTM), non-linear differential equations

MSC: 34A34, 34E05

Nomenclature

Symbols	Meaning
S_{E1}, S_{E2}	Dimensionless concentrations of substrates
P_{E1}, P_{E2}	Dimensionless concentratiosn of products
γ_1, γ_2	Dimensionless Reaction rate
y	Dimensionless space
S_{b1}, S_{b2}	Concentrations of substrates S_1, S_2 in Bulk solution (mol cm^{-3})
μ	Dimensionless constant
S_{e1}, S_{e2}	Concentrations of substrates S_1 and S_2 (mol cm^{-3})

$e1$, $e2$	Concentrations of substrates $E1$ and $E2$ (mol cm^{-3})
P_{e1}, P_{e2}	Concentrations of substrates P_1 and P_2 (mol cm^{-3})
$e1$, $e2$	Concentrations of substrates $E1$ and $E2$ (mol cm^{-3})
$D_{S_{e1}}$, $D_{S_{e2}}$, $D_{P_{e1}}$, $D_{P_{e2}}$	Diffusion coefficients within the enzyme layers (cm$^2 sec^{-1}$)
d	Distance between the electrode and enzyme layer(cm)

1. Introduction

Biosensors are sensing instruments that convert a biological interaction into an electrical output. An oxygen-sensitive electrode is a type of Biosensor designed to detect and measure oxygen concentration in a given solution. The oxygen electrode typically consists of a sensitive element that reacts with oxygen, generating a measurable signal as a current. Amperometric Biosensors detect the output current due to the electrochemical reaction [1–3]. While the Biosensor operates, the substrate being examined undergoes a biochemical transformation to produce a specific product. Typically, the Biosensor's response exhibits a direct relationship with the concentration of the reaction product [4]. Amperometric Biosensor find applications across various fields. Some of their notable applications include Biochemical applications, Environmental monitoring, the food and beverage industry, Biotechnology and Pharmaceuticals, Industrial applications, and wearable health devices [5, 6]. The development of mathematical models for enzyme Biosensors began with modelling the Amperometric enzyme electrode [7–10].

The unique characteristics of biosensors are essential for designing and enhancing them. Employing Mathematical modelling replaces physical experiments to improve the configuration for Biosensors. Effectively detailing the quantitative explanation of how reactions and diffusion occur within confined surface areas, as observed in Amperometric Biosensor systems, holds great significance. Baronas et al. developed a computational model that accurately simulates an amperometric biosensor using catalase-peroxidase-catalyzed two-substrate conversion through this approach. Additionally, it analyzes how various physical and kinetic parameters impact the Biosensor's response [11]. The exploration of Mathematical models for two-enzyme biosensors began with a focus on creating models for an Amperometric monolayer enzyme electrode containing two co-immobilized enzymes. Subsequent advancements led to the creation of non-linear mathematical models tailored for Amperometric two-enzyme biosensors utilizing varied enzyme combinations.

This study aims to create an analytical solution to the boundary value problem that defines how the Biosensor operates. This solution will depict the steady or non-steady concentration rates of the substances involved in the reaction, travelling through the catalytic layer based on distance and time. Analytical solutions for different kinds of biosensors have been documented in recent years. A straightforward Analytical expression is not available to determine the steady-state concentrations and current in an amperometric-based biosensor that uses parallel-substrate conversion within a biochemical reaction. Analytical methods such as Akbari-Ganji's Method (AGM) and Differential Transform Method (DTM) are applied to solve this model. The numerical results are gained using the Computational Software MATLAB. This paper introduces a straightforward and closed version of the Analytical expressions for determining substrate and product concentrations. These expressions are derived using a novel approach called the Akbari-Ganji Method (AGM).

2. Mathematical formulation of the problem

The catalase-peroxidase (parallel-substrate conversion) process can be used to describe the chemical reaction in the following manner.

$$S_1 \xrightarrow{E1} \frac{1}{2}P_1 \tag{1}$$

$$S_1 + S_2 \xrightarrow{E2} P_2 \qquad (2)$$
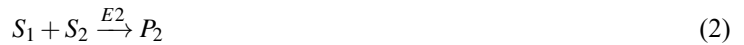
Two simultaneous conversions of two substrates (S_1 and S_2), to get resulting products (P_1 and P_2) utilizing two enzymes ($E1$ and $E2$) to accelerate the reaction. This Biosensor works in two parallel faces. Figure 1 illustrates the schematic depiction of the system. Combining the reactions catalyzed by catalase and peroxidase within the enzyme layer, as explained by Fick's law, results in formulating the reaction-diffusion equations that depict how the Biosensor operates within the enzyme layer as follows:

$$D_{S_{e1}} \frac{d^2 S_{e1}}{dx^2} = k_1 e1 S_{e1} + \frac{k_{21} k_{22} e2 S_{e1} S_{e2}}{k_{21} S_{e1} + k_{22} S_{e2}} \qquad (3)$$

$$D_{S_{e2}} \frac{d^2 S_{e2}}{dx^2} = \frac{k_{21} k_{22} e2 S_{e1} S_{e2}}{k_{21} S_{e1} + k_{22} S_{e2}} \qquad (4)$$

$$D_{P_{e1}} \frac{d^2 P_{e1}}{dx^2} = -\frac{k_1 e1 S_{e1}}{2} \qquad (5)$$

$$D_{P_{e2}} \frac{d^2 P_{e2}}{dx^2} = -\frac{k_{21} k_{22} e2 S_{e1} S_{e2}}{k_{21} S_{e1} + k_{22} S_{e2}} \qquad (6)$$
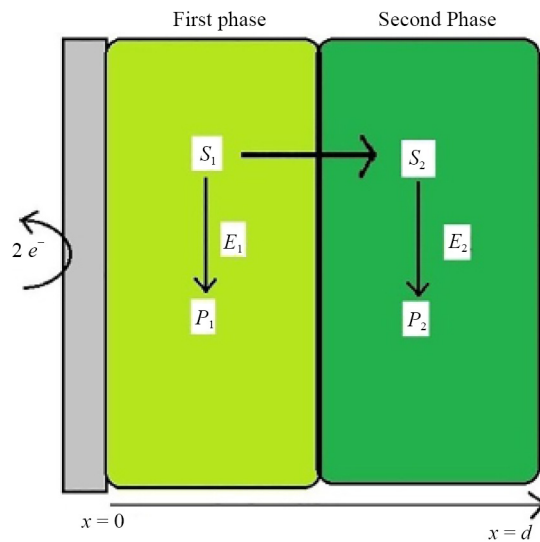

Figure 1. Schematic represeantation of the system

Where x stands for space. S_{e1}, S_{e2} are the concentration of substrates S_1 and S_2 and P_{e1}, P_{e2} are the concentration of products P_1 and P_2. $D_{S_{e1}}$, $D_{S_{e2}}$, $D_{P_{e1}}$, $D_{P_{e2}}$ are the corresponding diffusion coefficients and k_1, k_{21} and k_{22} are the reaction rate that occurs in the system. This Kinetic model Amperometric Biosensor has been developed under the following assumptions [12, 13].

✓ During the first stage of the Biosensor's function, the solution exclusively comprises hydrogen peroxide (S_1). When the Biosensor response stabilizes at the end of this initial phase. The second substrate(S_2) is introduced into the solution, initiating the second phase of the Biosensor's operation.

✓ The movements of substrates and product through diffusion happens beyond the enzyme layer, specifically in a region referred to as the Nernst diffusion layer.

✓ The boundary conditions of the system are given as follows.

$$D_{C_e}\left(\frac{dC_e}{dx}\right)_{x=0}, \ P_{e1}(x=0)=0, \ C=S_1, \ S_2, \ P_2 \tag{7}$$

$$S_{ei}(x=d)=S_{i0}, \ P_{ei}(x=d)=0, \ i=1, \ 2 \tag{8}$$

where d refers to the thickness of the enzyme layers.

✓ The steady-state non-dimensional form of the considered non-linear differential equations. Eqn (3), (4), (5), (6) are as follows.

$$\frac{d^2 S_{E1}}{dy^2}=\gamma_1 S_{E1}+\frac{\gamma_2 S_{E1} S_{E2}}{\mu S_{E1}+S_{E2}} \tag{9}$$

$$\frac{d^2 S_{E2}}{dy^2}=\gamma_2 \frac{S_{E1} S_{E2}}{\mu S_{E1}+S_{E2}} \tag{10}$$

$$\frac{d^2 P_{E1}}{dy^2}=-\gamma_1 \frac{S_{E1}}{2} \tag{11}$$

$$\frac{d^2 P_{E2}}{dy^2}=-\gamma_1 \frac{S_{E1} S_{E2}}{\mu S_{E1}+S_{E2}} \tag{12}$$

With the boundary conditions,

$$\frac{dS_{E1}}{dy}=\frac{dS_{E2}}{dy}=\frac{dP_{E2}}{dy}=0, \ P_{E1}=0 \ when \ y=0 \tag{13}$$

$$S_{E1}=S_{E2}=1, \ P_{E1}=P_{E2}=0 \ when \ y=1 \tag{14}$$

✓ With the dimensionless Parameters

$$S_{E1}=\frac{S_{e1}}{S_{b1}}, \ S_{E2}=\frac{S_{e2}}{S_{b2}}, \ P_{E1}=\frac{P_{e1}}{S_{b1}}, \ P_{E2}=\frac{P_{e2}}{S_{b1}}, \ y=\frac{x}{d}, \ \gamma_1=\frac{d^2 k_1 e1}{D_e}, \ \gamma_2=\frac{d^2 k_1^2 e2}{D_e}, \ \mu=\frac{S_{b1}}{S_{b2}} \tag{15}$$

✓ These equations were developed by assuming the model parameters [13] as,

$$D_{S_{e1}} = D_{S_{e2}} = D_{P_{e1}} = D_{P_{e2}} = D_e, \ and \ k_{21} = k_{22} = k_2 \tag{16}$$

✓ The dimensionless current response of the system is given by,

$$\psi = (\frac{dP_{E1}}{dy})_{y=0} \tag{17}$$

3. Approximate analytical expressions for the concentration of substrates and products using AGM

In general, non-linear systems do not possess precise analytical solutions. Researchers typically prefer analytical solutions as they offer a more lucid insight into how model parameters impact performance [14–17]. AGM has proven effective in addressing non-linear systems. AGM is an innovative approach of solving differential equations with algebraic expressions [18–22]. Many complex non-linear differential models encountered in science and engineering have been effectively addressed by utilizing the AGM. This method has proven its ability to provide highly accurate and approximate analytical solutions for these models. The detailed computation and analytical solution are given below, To solve the differential equations, it is assumed that the answers to the non-linear differential equations Eqn (9), (10) and (12) are as follows:

$$S_{E1}(y) = A cosh(my) + B sinh(my) \tag{18}$$

$$S_{E2}(y) = A_1 cosh(ny) + B_1 sinh(ny) \tag{19}$$

$$P_{E2}(y) = 1 - A_2 cosh(qy) + B_2 sinh(qy) \tag{20}$$

unknown coefficients A, A_1, A_2, B_1, B_2, n, m and q are obtained by applying the boundary conditions given in Eqns (13) and (14). The following are the approximate analytical solutions for the concentration of reactant species using AGM,

$$S_{E1}(y) = \frac{cosh(my)}{cosh(m)} \tag{21}$$

$$S_{E2}(y) = \frac{cosh(ny)}{cosh(n)} \tag{22}$$

$$P_{E2}(y) = 1 - \frac{cosh(qy)}{cosh(q)} \tag{23}$$

The Normalized current response of the system is derived as,

$$\psi = \frac{-\gamma_1}{2m^2}(\frac{1}{cosh(m)} - 1) \tag{24}$$

Where

$$m = \sqrt{\gamma_1 + \frac{\gamma_2}{\mu + 1}} \tag{25}$$

$$n = \sqrt{\frac{\gamma_2}{\mu + 1}} \tag{26}$$

$$q = \sqrt{\frac{\gamma_1}{1 + \mu}} \tag{27}$$

To solve eqn (11), substituting S_{E1} in eqn (11) we get,

$$\frac{d^2 P_{E1}}{dy^2} = \frac{-\gamma_1}{2} \frac{cosh(my)}{cosh(m)} \tag{28}$$

Now solving and applying the boundary condition we get,

$$P_{E1}(y) = \frac{-\gamma_1}{2} \left[\frac{cosh(my)}{cosh(m)} - \left(1 - \frac{1}{cosh(m)}\right)y - \frac{1}{cosh(m)} \right] \tag{29}$$

And the numeric values of the coefficients n, m and q are obtained using the reaction rate parameters γ_1, γ_2 and μ. For instance, for the particular values of parameter $\gamma_1 = 0.1$, $\gamma_2 = 0.1$ and $\mu = 5$. Solving Eqn (25), (26), (27). We get $m = 0.3415$, $n = 0.1291$, $q = 0.1291$.

4. Approximate analytical expressions for the concentration of substrates and products using DTM

In the year 1986, Zhou introduced DTM for solving differential equations. It is the extension of Taylor's series method. DTM approach is based on finding coefficients of Taylor's series. DTM is an existing method that provides a series expression of non-linear boundary value problems [23]. The detailed computation using DTM is given below, Considering the differential equation given in Eqn (9) with the initial conditions

$$\frac{dS_{E1}}{dy}(y = 0) = \frac{dS_{E2}}{dy}(y = 0) = 0 \tag{30}$$

The differential transformed form of Eqn (9) concerning the conditions given in Eqn (30) is given by,

$$((k+2)(k+1)s_1(k+2) - \gamma_1 s_1(k))(\mu s_1(k) + s_2(k)) - \gamma_2 \sum_{r=0}^{k} s_1(k)s_2(k-r) = 0 \tag{31}$$

$$s_1(1) = 0, \ s_2(1) = 0. \tag{32}$$

Now, Assume that,

$$s_1(0) = a, \ s_2(0) = b \tag{33}$$

Letting $k = 0$ in eqn (31), we get

$$(2s_1(2) - a\gamma_1)(\mu a + b) - ab\gamma_2 = 0 \tag{34}$$

$$\Rightarrow s_1(2) = \frac{a(a\gamma_1\mu + b\gamma_1 + b\gamma_2)}{2(\mu a + b)} \tag{35}$$

Now, taking the differential inverse transform $s_1(k)$ is defined as,

$$s_1(k) = \sum_{k=0}^{2} s_1(k)(y - y_0)^k \tag{36}$$

and letting $y_0 = 0$, we obtain the series expression solution as follows,

$$S_{E1}(y) = \sum_{k=0}^{2} s_1(k)(y)^k = a + \frac{a(a\gamma_1\mu + b\gamma_1 + b\gamma_2)}{2(\mu a + b)}y^2. \tag{37}$$

In a similar way we can find approximate analytical solutions for the concentration of reactant species using DTM, as follows:

$$S_{E1}(y) = a + \frac{a(a\gamma_1\mu + b\gamma_1 + b\gamma_2)}{2(\mu a + b)}y^2. \tag{38}$$

$$S_{E2}(y) = b + \frac{ab\gamma_2}{2(\mu a + b)}y^2 \tag{39}$$

$$P_{E1}(y) = cy - \frac{\gamma_1 a}{4}y^2 \tag{40}$$

$$P_{E2}(y) = f - \frac{ab\gamma_1}{2(\mu a + b)}y^2 \tag{41}$$

The Normalized current response of the system is derives as

$$\psi = c \tag{42}$$

The assumed constants a, b, c and f are obtained using the boundary condition given in Eqn (14). At $y = 1$ and for particular values of reaction-diffusion parameters $\gamma_1 = 0.1$, $\gamma_2 = 0.1$ and $\mu = 5$.

5. Comparison of analytical results with numerical simulation

In this Section, Numerical simulations are carried to evaluate how accurate and dependable the proposed method is. Recently, Mathematical modelling has been investigated with Numerical simulations [24–26]. The Mathematical expressions derived in this paper have been cross-referenced with a highly precise numerical solution acquired through MATLAB (pdex4) software. The code relevant to this is provided in Appendix A. Furthermore, the analysis involves comparing the numerical solutions with the AGM solutions Eqns (21) & (29) and the results are presented in the following tabular form.

6. Results and discussion

The amount of the specific substance present in it influences the Biosensor's reaction rate. Figure 2 shows that the AGM results are very close to the Numerical solution, and the DTM results have minor variation from the Numerical results. Therefore, Eqns (21), (22), (23) and (29) are the new simple and closed analytical expressions for the Normalized concentrations of Substrates (S_{E1}, S_{E2}) and Normalized concentrations of Products (P_{E1}, P_{E2}). Figure 3 depicts all the concentration curves verses dimensionless space.
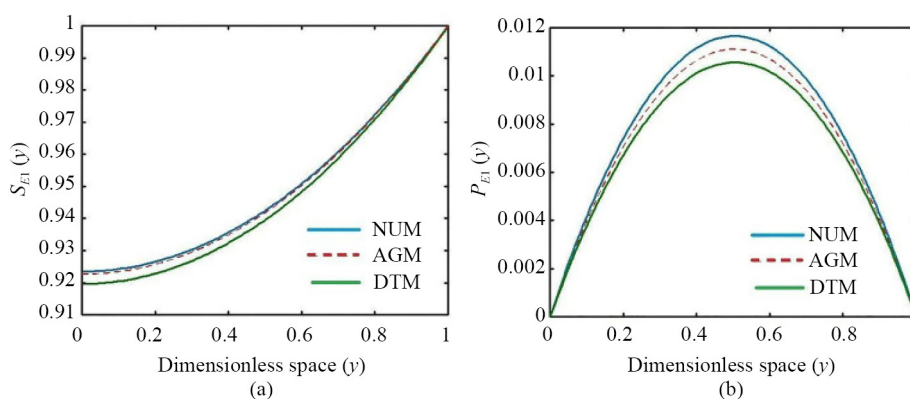

Figure 2. Comparison of AGM and DTM results with Numerical results (NUM)

The concentration profiles of the substrate and product within the enzyme layer, obtained through both analytical solution and computational simulation, are compared and displayed in Figure 3. The continuous line illustrates the analytical solution, while the dashed line represents the numerical solution. These particular curves were calculated using the subsequent standard parameter values, $\mu = 0.1$, $\gamma_1 = 0.1$, $\gamma_2 = 22$ for S_{E1}, $\mu = 5$, $\gamma_1 = 0.1$, $\gamma_2 = 20$ for S_{E2}, $\mu = 100$, $\gamma_1 = 100$, $\gamma_2 = 500$ for P_{E1}, $\mu = 100$, $\gamma_1 = 100$, $\gamma_2 = 100$ for P_{E2}. Both the calculated analytical and numerical solutions were represented on a shared graph, encompassing a broad spectrum of potential values for the highlighted parameters within the problem. Table 1 and 2 evidently shows an exceptional agreement between the analytical solution depicting reactant and product concentration profiles for the reaction-diffusion problem and the corresponding values obtained through numerical evaluation using MATLAB. On average, the variation between numerical and analytical outcomes is typically 0.39% for substrate (S_1) and 0.92% for product (P_1), indicating a highly accurate match.

Table 1. Comparison of the molar concentration of Substrate $S_1(S_{E1})$ given in Eqn (21) with Numerical (Num) result for the fixed value of parameter $\mu = 5$

y	$\gamma_1 = 0.1,\ \gamma_2 = 0.1$			$\gamma_1 = 0.1,\ \gamma_2 = 5$			$\gamma_1 = 1,\ \gamma_2 = 0.1$			$\gamma_1 = 5,\ \gamma_2 = 0.1$		
	Num Soln	AGM Soln	Error % of AGM	Num Soln	AGM Soln	Error % of AGM	Num Soln	AGM Soln	Error % of AGM	Num Soln	AGM Soln	Error % of AGM
0	0.944	0.944	0.02	0.657	0.664	1.13	0.642	0.643	0.20	0. 209	0.210	0.48
0.2	0.946	0.946	0.01	0.673	0.677	0.59	0.656	0.657	0.15	0.231	0.232	0.22
0.4	0.953	0.953	0.00	0.710	0.715	0.70	0.697	0.697	0.00	0.301	0.300	0.36
0.6	0.964	0.964	0.02	0.777	0.779	0.26	0.767	0.765	0.23	0.435	0.431	1.01
0.8	0.980	0.980	1.65	0.875	0.873	0.26	0.869	0.865	0.51	0.660	0.649	1.64
1	1.000	1.000	0.00	1.000	1.000	0.00	1.000	1.000	0.00	1.000	1.000	0.00
Avg error %		0.28			0.49			0.18			0.61	

Table 2. Comparison of the molar concentration of Substrate $P_1(P_{E1})$ given in Eqn (29) with Numerical (Num) result for the fixed value of parameter $\mu = 5$

| y	$\gamma_1 = 0.1,\ \gamma_2 = 0.1$			$\gamma_1 = 0.1,\ \gamma_2 = 5$			$\gamma_1 = 1,\ \gamma_2 = 0.1$			$\gamma_1 = 5,\ \gamma_2 = 0.1$		
	Num Soln	AGM Soln	Error % of AGM	Num Soln	AGM Soln	Error % of AGM	Num Soln	AGM Soln	Error % of AGM	Num Soln	AGM Soln	Error % of AGM
0	0.000	0.000	0.00	0.000	0.000	0.00	0.000	0.000	0.00	0.000	0.000	0.00
0.2	0.004	0.004	0.00	0.002	0.002	0.00	0.028	0.028	0.00	0.068	0.067	1.47
0.4	0.006	0.006	0.00	0.004	0.004	0.00	0.044	0.043	2.27	0.112	0.112	0.00
0.6	0.006	0.006	0.00	0.004	0.004	0.00	0.045	0.045	0.00	0.125	0.126	0.80
0.8	0.980	0.980	1.65	0.875	0.873	0.26	0.869	0.865	0.51	0.660	0.649	1.64
1	0.000	0.000	0.00	0.000	0.000	0.00	0.000	0.000	0.00	0.000	0.000	0.00
Avg error %		0.00			0.00			0.93			0.91	
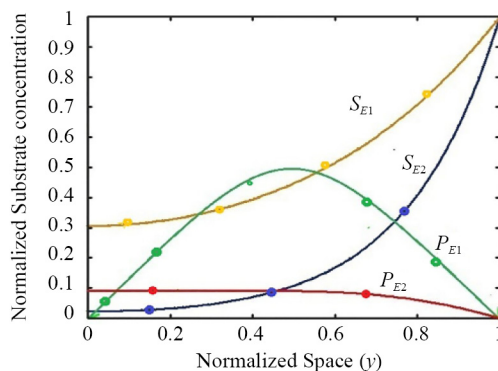
Figure 3. Plots between dimensionless concentration of Substrates (S_{E1}, S_{E2}) and dimensionless concentrations of Products (P_{E1}, P_{E2}) and space y

6.1 *Effect of parameter variation on substrate, product concentration and current*

Figure 4 displays the dimensionless concentration profiles of substrate (S_1), keeping the parameters μ, γ_2 as constant, adjust the reaction parameter γ_1 across different values. and Figure 5 displays the dimensionless concentration profiles of product (P_1), keeping the parameters μ, γ_1 as constant, adjust the reaction parameter γ_2 across different values. which are part of the Parallal-substrate conversion governed by reaction-diffusion equation given in Eqn (21) and Eqn (29). Observing the figure, it's evident that the analytical result we obtained aligns closely with the outcomes from numerical experiments. We have also analyzed the unique characteristics of the Biosensor activity by employing our analytical findings across different parameter values. As the rate of the reaction goes up, there is a corresponding rise in the concentration of the Product. The concentration of the substrate declines as the reaction rate increases. The Biosensor's present reaction is reliant on the concentration of the product (P_1). The analytical derivation provides the equation for the dimensionless current as expressed in Eqn (24). The current generated by the Biosensor is independent on the reaction rate. Instead, it steadily rises when reaction rate increases and decreases consistently as reaction rate γ_1 increases. It is displayed in Figure 6, keeping the parameters as constant, adjust the reaction parameter γ_1 and γ_2 across different values. This work may extend for predicting biosensor response with multi-substrate conversion and biosensor with substrate inhibition. And also, the Mathematical formulation can be developed for the enzyme electrode with different shapes.
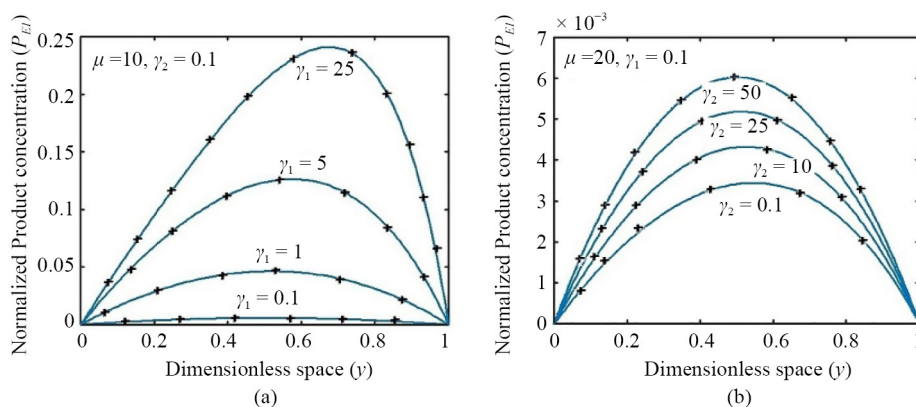

Figure 4. Plots between dimensionless concentration of First Product (S_{E1}) and dimension space y
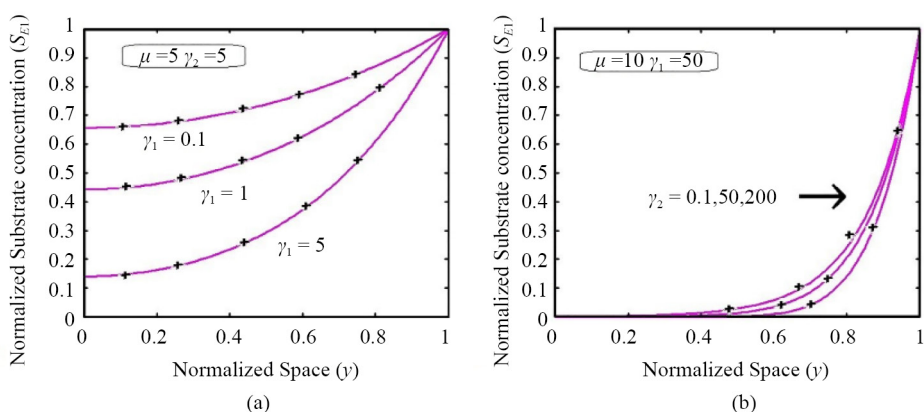

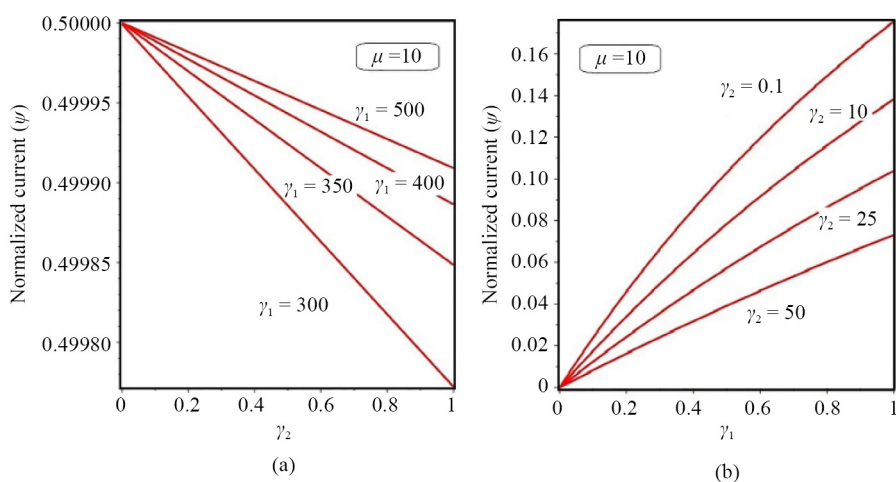**Figure 5.** Plots between dimensionless concentration of First Product (P_{E1}) and dimension space y

Contemporary Mathematics

Figure 6. Plots between dimensionless reaction parameter (γ_1, γ_2) and dimensionless current (ψ)

7. Conclusions

A Mathematical representation illustrating the steady-state reaction behaviour of an amperometric biosensor that operates using catalase-peroxidase biochemical reactions (parallel-substrate conversion) is presented. A coupled non-linear Differential Equations has been effectively addressed by applying a novel technique known as the AGM. The obtained analytical expressions offer a simple, straightforward and more effective means to grasp and anticipate how the system will behave. The results obtained from our analytical approach, which solves for the substrates and resulting products, have been verified against a numerical method, showing reliable and matching outcomes. The Biosensor current response concerning the kinetic parameters is also discussed.

Conflict of interest

Authors declare there is no conflict of interest at any point with reference to research findings.

References

[1] Lojou E, Bianco P. Application of the electrochemical concepts and techniques to amperometric biosensor devices. *Journal of Electroceramics*. 2006; 16: 79-91. Available from: doi:10.1007/s10832-006-2365-9.

[2] Bollella P, Gorton L. Enzyme based amperometric biosensors. *Current Opinion in Electrochemistry*. 2018; 10: 157-173. Available from: doi:10.1016/j.coelec.2018.06.003.

[3] Prodromidis M, Karayannis M. Enzyme based amperometric biosensors for food analysis. *Electroanalysis*. 2022; 14(4): 241-261.

[4] Kulys J, Krikstopaitis K, Ziemys A. Kinetics and thermodynamics of peroxidase- and laccase-catalyzed oxidation of N-substituted phenothiazines and phenoxazines. *Journal of Biological Inorganic Chemistry*. 2000; 5: 333-340. Available from: doi:10.1007/PL00010662.

[5] Irfan J, Raza A, Ali M. Biosensors: Their fundamentals, designs, types and most recent impactful applications: A review. *Journal of Biosensors Bioelectronics*. 2017; 8(1): 1000235.

[6] Cinti S, Volpe G, Piermarini S, Delibato E, Palleschi G. Electrochemical biosensors for rapid dedection of foodborne Salmonella: A criticle overview. *Sensors*. 2017; 17(8): 1910.

[7] Kulys J, Sorochinskii V, Vidziunaite R. Transient response of bienzyme electrodes. *Biosensors*. 1986; 2(3): 135-146.

[8]   Sorochinskii VV. Steady-state kinetics of cyclic conversions of substrate in amperometric bienzyme sensors. *Biosensors and Bioelectronics*. 1996; 11(3): 225-238.

[9]   Ferreira LS, de Souza Jr MB, Trierweiler JO, Broxtermann O, Folly ROM, Hitzmann B. Aspects concerning the use of biosensors for process control: Experimental and simulation investigations. *Computers Chemical Engineering*. 2023; 27(8-9): 1165-1173.

[10] Baronas R, Feliksas I, Juozas K. The influence of the enzyme membrane thickness on the response of amperometric biosensors. *Sensors*. 2003; 3(7): 248-262.

[11] Ašeris V, Baronas R, Kulys J. Modelling the Biosensor utilizing parallel substrates conversion. *Journal of Electroanalytical Chemistry*. 2012; 685: 63-71. Available from: doi:10.1016/j.jelechem.2012.06.025.

[12] Andersen M, Hsuanyu Y, Welinder K, Schneider P, Frøystein N, Francis G, et al. Spectral and kinetic properties of oxidized intermediates of coprinus cinereus peroxidase. *Acta Chemica Scandinavica-ACTA Chem Scand*. 1991; 45: 1080-1086. Available from: doi:110.3891/acta.chem.scand.45-1080.

[13] Rajendran L, Saranya K, Mohan V, Narayanan KRS. Reaction/diffusion equation with michaelis-menten kinetics in microdisk biosensor: Homotopy perturbation method approach. *International Journal of Electrochemical Science*. 2019; 14(2019): 3777-3791.

[14] Reena A, Karpagavalli SG, Rajendran L, Manimegalai B, Swaminathan R. Theoretical analysis of putrescine enzymatic biosensor with optical oxygen transducer in sensitive layer using Akbari-Ganji method. *International Journal of Electrochemical Science*. 2021; 18(5): 100113.

[15] Tawanda T, Nyamugure P, Kumar S, Munapo E. An intelligent node labelling maximum flow algorithm. *International Journal of System Assurance Engineering and Management*. 2023; 14(4): 1276-1284.

[16] Swaminathan R. Analytical solution of non linear problems in homogeneous reactions occur in the masstransfer boundary layer: Homotopy perturbation method. *International Journal of Electrochemical Science*. 2021; 16(6): 210644

[17] Mothilal K, Sivasankari M, Vellaiammal R, Rajendran L. Theoretical analysis of concentration of lactose hydrolysis in a packed bed reactor using immobilized β-galactosidase. *Ain Shams Engineering Journal*. 2018; 9(4): 1507-1512.

[18] Nebiyal A, Swaminathan R, Karpagavalli SG. Reaction kinetics of Amperometric enzyme electrode in various geometries using the Akbari-Ganji method. *International Journal of Electrochemical Science*. 2023; 18(9): 100240.

[19] Ranjani K, Swaminathan R, Karpagavalli SG. Mathematical modelling of a mono-enzyme dual amperometric biosensor for enzyme-catalyzed reactions using homotopy analysis and akbari-ganji methods. *International Journal of Electrochemical Science*. 2023; 18(9): 100220.

[20] Pirabaharan P, Devi MC, Swaminathan R, Rajendran L, Lyons MEG. Modelling the current response and sensitivity of oxidase enzyme electrodes, monitored amperometrically by the consumption of oxygen. *Electrochem*. 2022; 3(2): 309-321.

[21] Reena A, Karpagavalli S, Swaminathan R. Theoretical analysis and steady-state responses of the multienzyme amperometric biosensor system for nonlinear reaction-diffusion equations. *International Journal of Electrochemical Science*. 2023; 18(10): 100293.

[22] Ranjani K, Swaminathan R, Karpagavalli SG. A theoretical investigation of steady-state concentration processes at a carrier-mediated transport model using Akbari-Ganji and differential transform methods. *Partial Differential Equations in Applied Mathematics*. 2023; 8: 100594. Available from: doi:10.1016/j.padiff.2023.100594.

[23] Arikoglu A, Ozkol I. Solution of differential-difference equations by using differential transform method. *Applied Mathematics and Computation*. 2006; 174(2): 153-162.

[24] Jahan S, Ahmed S, Yadav P, Nisar K. Fibonacci wavelet method for the numerical solution of a fractional relaxation-oscillation model. *Partial Differential Equations in Applied Mathematics*. 2023; 8: 100568. Available from: doi:10.1016/j.padiff.2023.100568.

[25] Yadav P, Jahan S, Nisar KS. Fractional order mathematical model of Ebola virus under Atangana-Baleanu- Caputo operator. *Results in Control and Optimization*. 2023; 13: 100332. Available from: doi:10.1016/j.rico.2023.100332.

[26] Nebiyal A, Swaminathan R, Karpagavalli SG. Mathematical modelling and application of analytical methods for a nonlinear ec2e mechanism in rotating disk electrode. *International Journal of Analysis and Applications*. 2024; 22(92): 1-16.

Appendix A

```
Function nebi
m = 0;
x = linspace (0, 1);
t = linspace(0, 10000000000);
sol = pdepe(m, @pdex4pde, @pdex4ic, @pdex4bc, x, t);
u1 = sol(:, :, 1);
u2 = sol(:, :, 2);
u3 = sol(:, :, 3);
u4 = sol(:, :, 4);
figure
plot(x, u1(end, :))
title('u1(x, t)')
function [c, f, s] = pdex4pde(x, t, u, DuDx)
c = [0; 0; 0; 0];
f = [1; 1; 1; 1].* DuDx;
r1 = 0.1; r2 =0.1 ; mu = 5;
F1 = - r1 * u(1) - (r2 * u(1) * u(2))/(mu * u(1)+u(2) );
F2 = - (r2 * u(1) * u(2))/(mu * u(1)+u(2));
F3 = ((r1/2) * u(1));
F4 = (r1 * u(1) * u(2))/(mu * u(1)+u(2));
s = [F1; F2; F3; F4]; function u0 = pdex4ic(x)
u0 = [1; 1; 0; 0];
function [pl, ql, pr, qr]= pdex4bc(xl, ul, xr, ur, t)
pl = [0; 0; ul(3); 0];
ql = [1; 1; 0; 1];
pr = [ur(1)-1; ur(2)-1; ur(3)-0; ur(4)-0];
qr = [0; 0; 0; 0];
```